

†Research sponsored jointly by the National Science Foundation and U. S. Atomic Energy Commission under contract with Union Carbide Corp.

\*Guest scientist from Physics Department, West Virginia Univ., Morgantown, W. Va. 26506.

<sup>1</sup>J. H. Schulman and W. D. Compton, *Color Centers in Solids* (MacMillan, New York, 1962).

<sup>2</sup>J. H. Crawford, *Advan. Phys.* **17**, 93 (1968).

<sup>3</sup>E. Sonder and W. A. Sibley, in *Defects in Solids*, edited by J. H. Crawford and L. Slifkin (Plenum, New York, 1972).

<sup>4</sup>B. Henderson and J. E. Wertz, *Advan. Phys.* **17**, 749 (1968).

<sup>5</sup>A. E. Hughes and B. Henderson, in Ref. 3.

<sup>6</sup>P. Gorlich, H. Karras, Ch. Symanowski, and P. Ukman, *Phys. Status Solidi* **25**, 92 (1968).

<sup>7</sup>W. A. Sibley and O. E. Facey, *Phys. Rev.* **174**, 1076 (1968).

<sup>8</sup>T. P. P. Hall and A. Leggeat, *Solid State Commun.* **7**, 1657 (1969).

<sup>9</sup>C. R. Riley and W. A. Sibley, *Phys. Rev. B* **1**, 2789 (1970).

<sup>10</sup>C. R. Riley, Ph.D. dissertation (University of Tennessee, 1970) (unpublished).

<sup>11</sup>A. E. Hughes (private communication).

<sup>12</sup>D. Pooley, *Solid State Commun.* **4**, 351 (1965); *Proc. Phys. Soc. (London)* **87**, 245 (1966); 247 (1966).

<sup>13</sup>W. E. Vehse, F. Sherrill, and C. R. Riley, *J. Appl. Phys.* **43**, 1320 (1972).

<sup>14</sup>All percentages refer to the fraction of Mg and Mn sites occupied by Mn ions. Stated another way, the values quoted are the mole percentages of  $\text{KMnF}_3$  in mixture.

<sup>15</sup>E. Sonder and W. A. Sibley, *Phys. Rev.* **140**, A539 (1965).

<sup>16</sup>W. D. Compton and H. Rabin, in *Solid State Physics*, edited by F. Seitz and D. Turnbull, (Academic, New York, 1963), Vol. 16.

<sup>17</sup>P. B. Still and D. Pooley, *Phys. Status Solidi* **32**, 147K (1969).

<sup>18</sup>J. Ferguson, H. J. Guggenheim, and Y. Tanabe, *J. Phys. Soc. Japan* **21**, 692 (1965).

<sup>19</sup>F. A. Cotton, *Chemical Applications of Group Theory* (Wiley, New York, 1963).

## Coloration Induced in MgO by MeV $^{20}\text{Ne}^+$ Bombardment

Bruce D. Evans, James Comas, and Philip R. Malmberg

*Naval Research Laboratory, Washington, D. C. 20390*

(Received 13 March 1972)

The coloration produced near room temperature in MgO by 1.0- to 4.8-MeV  $^{20}\text{Ne}^+$  bombardment has been investigated. Energetic  $\text{Ne}^+$  ions incident upon crystalline MgO induce point defects on the anion sublattice primarily through atomic collisions. An electron(s) trapped in the anion vacancy forms an *F*-type center producing a characteristic, intense optical-absorption band near 5 eV. This point-defect lattice damage is restricted primarily to a thin layer of material approximately 1 to 2  $\mu$  thick located 2 to 4  $\mu$  beneath the bombarded surface. Average *F*-type-center volume concentrations in this thin layer range from  $4 \times 10^{18}$  to  $5 \times 10^{19} \text{ cm}^{-3}$  resulting from a  $\text{Ne}^+$  dose range of  $10^{13}$  to  $3 \times 10^{16} \text{ ions/cm}^2$ . *F*-type-center production is relatively inefficient; it is estimated that 5 keV are expended per center produced, in the low-dose range, assuming centers are created only by atomic collision processes. The peak *F*-type-center volume concentration saturates near  $10^{20} \text{ cm}^{-3}$  resulting from a dose of  $10^{16} \text{ ions/cm}^2$  at 3-MeV energy. This concentration level is followed by a decrease upon subsequent bombardment. A similar saturation effect is observed for a 574-nm absorption band. A quadratic dependence between the growth of the intensity of the *F*-type center and that of the 574-nm band suggests the latter is associated with a divacancy. Volume-concentration saturation levels for both bands are independent of many impurities commonly present in this material. Isochronal annealing results demonstrate that both bands have annealed out at 600 °C. Comparison is made with previously reported fast-neutron irradiations and the present work. Point defects on the cation sublattice, such as the *V*<sup>-</sup> center, were sought for but determined not to be present in sufficient concentration to be detected by the presence of the well-known 2.3-eV optical-absorption band.

### I. INTRODUCTION

Radiation damage in MgO has been studied extensively by several workers during the past decade.<sup>1-3</sup> Both Van de Graaff electron irradiation and fast-neutron irradiation produce an intense optical-absorption band near 250 nm. This band has been assigned to an *F*-like center. More care-

ful work by Kappers, Kroes, and Hensley<sup>4</sup> has shown that the 250-nm band is in fact composed of two closely spaced bands, one at 250.0 nm and the other at 246.5 nm measured at 80 °K. The former is assigned to the *F*<sup>+</sup> center, one electron trapped at an oxygen vacancy,<sup>3</sup> the latter to the *F* center, two electrons trapped at an oxygen vacancy. Since these two centers are different

charge states of the same lattice defect and since their principal absorption bands are indistinguishable in the present data, we will in this paper simply relate the composite 250-nm band to an *F*-type center. Fast-neutron irradiation produces other characteristic optical bands at 355, 574, and 975 nm.<sup>5</sup> The centers responsible for these bands have not been positively identified.

Henderson and King<sup>6</sup> have reported the growth of the *F*-type-center concentration with increasing fast-neutron ( $E > 1$  MeV) dose. More recent results by Chen *et al.*<sup>5</sup> cover the fast-neutron dose range of  $10^{15}$  to  $6 \times 10^{18}$  neutrons/cm<sup>2</sup>. We have studied the volume concentration of *F*-type centers induced in single crystal MgO by <sup>20</sup>Ne<sup>+</sup> ion bombardment.

During their passage through matter, energetic ions lose energy through two mechanisms: (a) ionizing target atoms (electronic energy loss) and (b) by nuclear collisions producing secondary energetic ions. These secondary ions may undergo similar nuclear collisions producing tertiaries, etc., resulting in a displacement cascade. A description of the slowing down of energetic ions in materials has been given by Lindhard, Scharff, and Schiott,<sup>7</sup> referred to as the LSS theory. While the ionization-energy-loss process may contribute to Frenkel defect production in such materials as the alkali halides, we show below that for MgO at low and moderate doses, atomic collision processes dominate defect production during room-temperature ion bombardment. Since an appreciable portion of the energy of the incident ion is deposited through atomic collisions within a few microns beneath the target surface, extremely high levels of lattice damage are produced within a very thin layer. It is then possible to study defect densities and saturation effects via optical-absorption spectroscopy in MgO samples which otherwise would be too opaque if uniformly damaged as by fast neutrons. By obtaining an equivalent fast-neutron dose in terms of employed ion doses, we are able to extend optical measurements for an equivalent fast-neutron dose in excess of  $10^{21}$  neutrons/cm<sup>2</sup>. At these high equivalent doses saturation effects are observed for both the *F*-type center and a possible *F*-aggregate center (574-nm band).

## II. PROCEDURE

### A. Experimental

Single crystals of MgO were used.<sup>8</sup> A typical impurity analysis is shown in Table I. Ultrahigh-purity MgO crystals were also used.<sup>9</sup> Growth, impurity analysis, and characterization of this material were made by Butler *et al.*<sup>10</sup> Small  $8 \times 9$  mm<sup>2</sup> platelets were cleaved parallel to the

(100) face and ground and polished to approximately 0.5 mm thickness.

The NRL 5-MV Van de Graaff accelerator was used to produce the 1.0 to 4.8-MeV beams of <sup>20</sup>Ne<sup>+</sup> ions with which samples were irradiated. The error associated with incident ion energies was less than 2%. The beams were magnetically analyzed and the beam spots electrostatically scanned over an area larger than the samples (approximately  $2 \times 2.5$  cm) in order to provide uniform irradiations. Secondary electrons produced at the brass mounting plate around the periphery of the target served to prevent surface charge buildup. The beam current on target was measured and integrated in a Faraday cup arrangement fitted with a negatively biased guard ring at its entrance to suppress secondary electrons. Beam currents were typically 0.5  $\mu$ A, although higher-dose runs employed a 2.5- $\mu$ A beam. The area bombarded, well defined by a rectangular aperture, was measured and used together with the integrated beam charge to calculate the total number of ions per cm<sup>2</sup> incident on the sample. The accumulated error in dose was estimated to be  $\pm 15\%$ . Samples were placed off axis to eliminate the possibility of a neutral beam component striking them. Such an unscanned neutral component would produce lattice damage but would not be measured as part of the incident beam current.

Ne<sup>+</sup> was initially chosen as the incident ion for two reasons: First, the mass ratio of incident ion to target atom determines the maximum energy transferred in an elastic atomic collision, and <sup>20</sup>Ne gives the best mass match for an MgO target of all the noble gases. Lighter ions, such as H<sup>+</sup> and He<sup>+</sup>, at the same incident energy as Ne<sup>+</sup>, lose more energy through nonvacancy-forming electronic collisions. Second, the noble gases are expected to be the least likely to enter into chemical bonding with the target constituents and are not anticipated to be optically active in the near-infrared, visible, and near-ultraviolet spectrum. This diminishes the possibility of interference from complex absorption spectra originating with the implanted species.

Samples were held with metal clips onto a  $\frac{1}{2}$ -in.-thick brass end plate. By exposing a small test

TABLE I. MgO impurity analysis (Refs. 8 and 10).

Element	Impurity constant ( $\mu$ g/g)
Al	1-10
Ca	100
Cu	10
Fe	30-100
Mn	10-100
Si	20-100
Ti	<20

sample mounted at the end of a wire thermocouple to a high beam flux and by considering the mounting arrangement for used samples, the maximum possible sample temperature during irradiation was estimated to be 70 °C.

Optical measurements were performed with a Cary model No. 14MR recording spectrophotometer. A small cryostat was used for low-temperature measurements. Infrared measurements were taken with a Perkin-Elmer model No. 521 grating infrared spectrometer fitted with a  $1 \times 4$  refracting beam condenser with KBr lenses. Some optical measurements were taken within half an hour of removal from the Van de Graaff. After 6 months storage at room temperature the same samples were checked again for absorbance. There was no noticeable change over this time span.

Isochronal annealing results were obtained by the following procedure. Samples were held at a fixed, elevated temperature for 12 min in a dry-nitrogen atmosphere. They were then placed on an aluminum block in air and quickly returned to room temperature within a few minutes. Absorption measurements were then taken at room temperature. This cycle was repeated several times, each time returning to a successively higher temperature, until the coloration was removed.

The procedure and results for obtaining  $F$ -type-center volume-concentration profiles in ion-irradiated samples will be discussed fully elsewhere. It may serve here to mention that the absorbance of the 250-nm band was monitored as successive layers of material were chemically removed.<sup>11</sup> The etch rates for both the bombarded and virgin sample regions were determined by multiple-beam interferometric measurements<sup>12</sup> which afforded a depth resolution of approximately 0.03  $\mu$ . Absorbance was converted to  $F$ -type-center volume concentration  $N_F$  by Dexter's<sup>13</sup> form of Smakula's formula

$$N_F f = (0.87 \times 10^{17}) [n / (2 + n^2)^2] \alpha_{\max} \Delta E, \quad (1)$$

where  $f$  is the oscillator strength 0.8,  $n$  the index of refraction of the host material,  $\Delta E$  the absorption band full width at half-peak height, and  $\alpha_{\max}$  is the absorption coefficient at the band peak.

#### B. Correlation of Fast-Neutron and Heavy-Ion Lattice Damage

In relating the level of lattice induced by fast-neutron irradiation to that produced by heavy-ion bombardment, two considerations arise which will be dealt with separately. They are first, putting the ion fluence on an equivalent footing with that for fast neutrons in terms of damage produced to the lattice per unit volume and per incident particle, and second, presenting all lattice-damage

data in terms of concentration of displacements per unit volume instead of numbers of displacements per square or absorbance. This latter factor is important because we will be comparing a relatively uniform spacial distribution (over several millimeters) of  $F$ -type centers induced by fast-neutron irradiation with a very distinct spatial profile of  $F$ -type centers restricted within a few microns of the bombarded surface induced by heavy-ion bombardment. This accumulation of lattice damage near the end of the incident ion's trajectory is a result of the well-known Bragg peak in nuclear stopping power.<sup>7</sup>

First we compare the number of displacements created per unit volume at a distance  $x$  beneath the irradiated surface per unit neutron fluence with the same number per unit volume at  $x$ ,  $N_d(x)$ , per unit ion fluence for given incident neutron and ion energies. Following Kulcinski, Laidler, and Doran,<sup>14</sup> using the Kinchin-Pease approximation,<sup>15</sup> the former is approximately  $10^2 \text{ cm}^{-1}$ . The latter may be estimated from

$$N_d(x) = \frac{1}{2E_d} \left( \frac{dE}{dR} \right)_{n_d} \Phi_i, \quad (2)$$

where  $[(dE/dR)(x)]_{n_d}$  is the distributed specific nuclear energy loss,  $\Phi_i$  the ion fluence, and  $E_d$  the displacement threshold energy.  $E_d$  for an oxygen atom in crystalline MgO has been measured by Chen *et al.*<sup>16</sup> by 0.23- to 29-MeV electron irradiation. They find  $E_d = 60 \text{ eV}$ . Again following Kulcinski *et al.*,<sup>14</sup> an estimate of the distributed specific nuclear energy loss is obtained from the specific nuclear-energy loss  $[(dE/dR)(x)]_n$  derived from LSS theory, by convoluting with a Gaussian distribution of projected ranges.<sup>17</sup> This approximation assumes the Gaussian parameter  $\sigma$  to be a constant. It is equal to the projected range standard deviation for a particle ( $\text{Ne}^+$ ) with energy  $E$  (here  $E = 3 \text{ MeV}$ ) incident onto MgO and is obtained from an extended<sup>18</sup> Johnson-Gibbons-type<sup>19</sup> computer code for the LSS theory.<sup>7</sup> Figure 1 shows these stopping powers for the special case of 3-MeV  $\text{Ne}^+$  incident on an MgO target. Substitution of a median value of distributed nuclear stopping power (0.12 MeV/ $\mu$  from Fig. 1) into Eq. (2) yields a value for  $N_d/\Phi_i$  of approximately  $10^7 \text{ cm}^{-1}$ . The important result here is that the fast-neutron dose, resulting in a uniform spatial distribution of defects, must be approximately  $10^5$  times greater than the  $\text{Ne}^+$  dose required to simulate the same "average" level of lattice damage restricted within a very thin layer of MgO just below the bombarded surface. For example, we find that a 3-MeV  $\text{Ne}^+$  fluence of  $10^{15} \text{ ions/cm}^2$  is equivalent to a fast-neutron fluence of approximately  $10^{20} \text{ neutrons/cm}^2$  in terms of the "average" number of lattice displacements expected per unit volume.

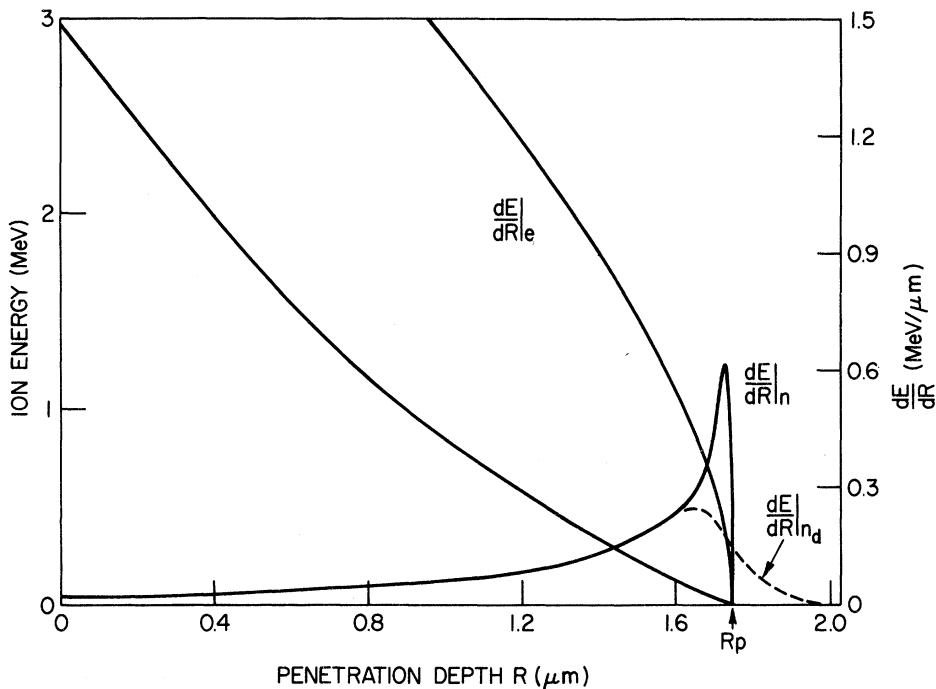


FIG. 1. Theoretical results of LSS for the slowing down of 3-MeV  $\text{Ne}^+$  ions incident on an MgO target. The left-hand curve shows the penetration depth as a function of energy for the "average" particle. On the right are shown stopping powers for both electronic  $(dE/dR)_e$  and nuclear, processes  $(dE/dR)_n$  again for the "average" particle. The distributed nuclear stopping power  $(dE/dR)_{nd}$  calculated by the method of Kulcinski, Laidler, and Doran, assuming a Gaussian distribution of ranges, is shown as the dashed curve.

### III. RESULTS

#### A. Coloration Induced by Ion Bombardment

Figure 2 shows the optical absorption in MgO induced by 3-MeV  $\text{Ne}^+$  ion bombardment. The major band near 5.0 eV (250 nm) is associated with the F-type center.<sup>1</sup> The weak band near 2.2 eV (574 nm) is also shown in the insert on an expanded scale. As depicted in Fig. 2 these two bands are also seen

in fast-neutron irradiated MgO.<sup>1,5</sup> The weak inflections near 4.3 and 5.7 eV are the well-known charge-transfer bands<sup>20,21</sup> originating with  $\text{Fe}^{+3}$ . Evidently incident ions are ionizing impurities such as iron:  $\text{Fe}^{+2} \rightarrow \text{Fe}^{+3} + e^-$ . This is evidenced by the fact that the weak iron band was observed to grow with increasing ion dose. Furthermore, at the end of the etching procedure when the 5-eV band had vanished completely, the original prebombard-

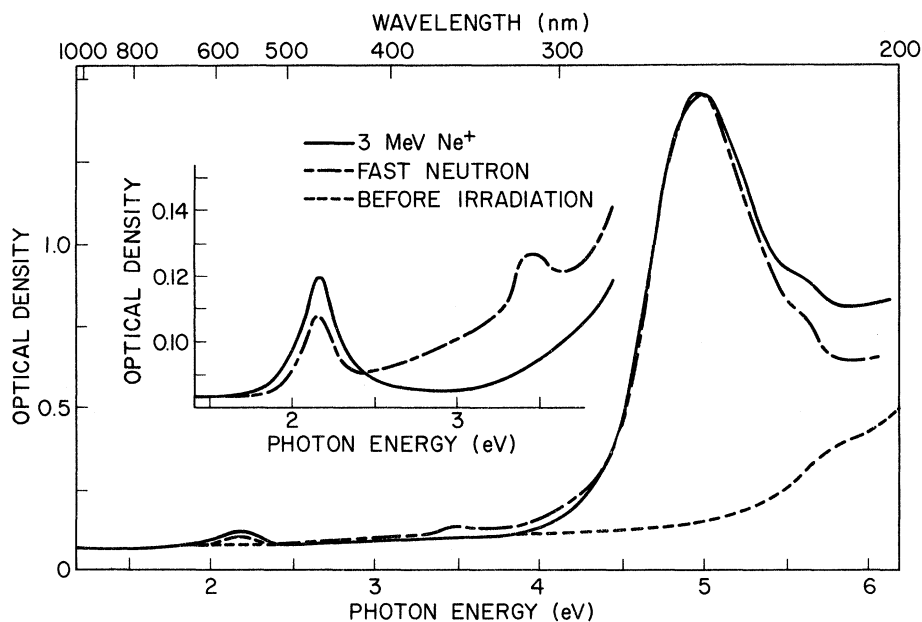


FIG. 2. Comparison of room-temperature absorption spectrum induced in crystalline MgO (General Electrical material) by fast-neutron irradiation with that produced by 3-MeV  $\text{Ne}^+$  bombardment. The ion spectrum shown resulted from a dose of  $3.5 \times 10^{15}$  ions/cm<sup>2</sup>. Neutron-irradiated samples were obtained from J. Kemp. The fast-neutron spectrum was normalized to the ion spectrum so that the F-band maxima coincided. The original neutron sample absorbance at 250-nm was 3.2 OD (optical density). No corrections were made for reflection losses.

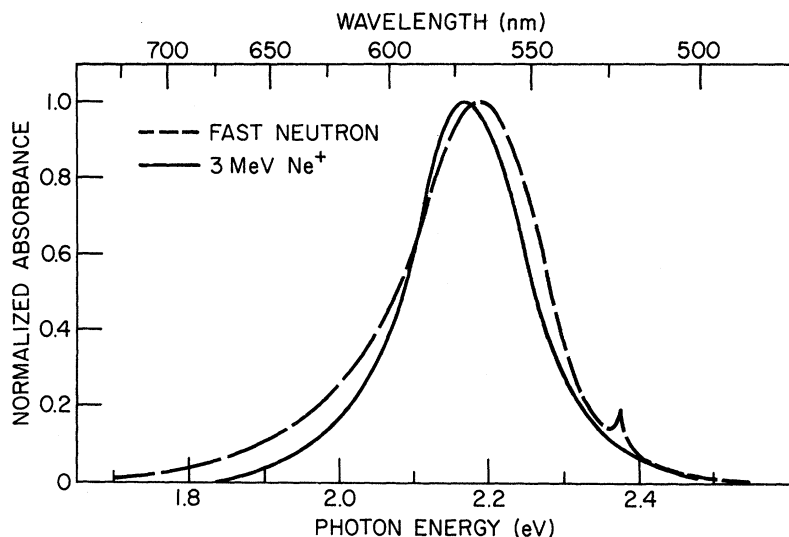


FIG. 3. Normalized comparison of the 574-nm band at 80 °K induced by fast-neutron irradiation with that produced by 3-MeV  $\text{Ne}^+$  bombardment to a dose of  $3.5 \times 10^{16}$  ions/cm<sup>2</sup>.

ed sample absorption spectrum was recovered.

Figure 3 compares the shape of the 574-nm band near 80 °K in both neutron-irradiated and ion-bombarded MgO. Our measurements for both cases indicate that the ion-irradiated band maximum appears at a slightly lower energy ( $2.165 \pm 0.006$  vs  $2.190 \pm 0.006$  eV); this is true for both the General Electric and Oak Ridge materials. This discrepancy is not surprising in view of the fact that Chen and Sibley<sup>22</sup> have suggested that this broad 574-nm band may be a composite of several bands and its peak position dependent upon past thermal history. The line near  $2.375 \pm 0.006$  eV in the fast-neutron irradiated material has been shown to have trigonal symmetry<sup>23</sup> in the (111) plane and is believed to consist of three neighboring anion vacancies. Furthermore, it is believed to be a five-electron center possessing a single trapped hole. This line is as-

signed to the  $R_3$  center by Glaze and Kemp.<sup>24</sup> It is interesting that we do not see this  $R_3$ -center line in  $\text{Ne}^+$  irradiated MgO, although strains introduced by the relatively high damage level may broaden this narrow line. No other  $\text{Ne}^+$  bombardment induced bands were detected in the range 1–11  $\mu$ .

#### B. Simulation and Extension of Fast-Neutron Lattice Damage in MgO with $\text{Ne}^+$ Bombardment

In order to relate lattice damage induced by energetic ion bombardment to that produced by fast neutrons, an experimental determination of volume concentration of defects produced by the  $\text{Ne}^+$  bombardment must be made. A typical result from successive etching and absorption measurements by which this information was obtained is shown in Fig. 4 for the case of a 3-MeV  $\text{Ne}^+$  ion dose of  $1.2 \times 10^{14}$  ions/cm<sup>2</sup>. The  $F$ -type-center volume

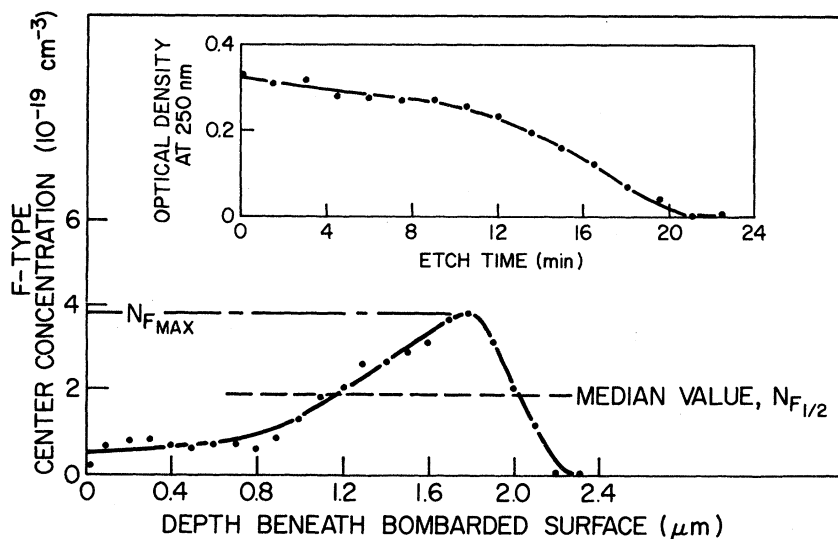


FIG. 4. Experimental  $F$ -type-center volume-concentration profile obtained in MgO from 3-MeV  $\text{Ne}^+$  bombardment to a dose of  $1.2 \times 10^{14}$  ions/cm<sup>2</sup>. This sample was aligned such that during bombardment the ion beam was incident ( $0.4 \pm 0.1$ )° from the  $\langle 100 \rangle$  direction. The crystal direction was determined on samples from x-ray back-reflection Laue patterns.

concentration is not uniform; it rises to a maximum some distance into the material near the particle's end path. The  $F$ -type-center volume concentration ranges from  $0.5 \times 10^{19} \text{ cm}^{-3}$  at the irradiated surface to a maximum of  $3.8 \times 10^{19} \text{ cm}^{-3}$ . For comparison we choose a median value ( $N_{F_{1/2}}$ ) of approximately  $2 \times 10^{19} \text{ cm}^{-3}$   $F$ -type centers resulting from a dose of  $1.2 \times 10^{14}$  ions/cm<sup>2</sup>. Using the  $10^5$  factor (Sec. II) for the equivalent fast-neutron dose, we find this median concentration would have been produced by an equivalent fast-neutron fluence of approximately  $10^{19}$  neutrons/cm<sup>2</sup>. We caution that this result is approximate, most probably accurate to an order of magnitude. Several other MgO samples exposed to 3-MeV Ne<sup>+</sup> beams within the dose range of  $10^{13}$  to  $3 \times 10^{16}$  ions/cm<sup>2</sup> were treated in a similar manner. These results are shown in Fig. 5 together with the fast-neutron results of Chen *et al.*<sup>5</sup> The upper dashed line in Fig. 5 represents volume concentration-vs-ion-dose data using the peak concentrations  $N_{F_{\text{max}}}$  (see Fig. 4) while the lower dashed line is formed from data using the volume concentrations at the bombarded surface  $N_{F_{\text{min}}}$ . These dashed lines then enclose a range of  $F$ -type-center concentration induced by Ne<sup>+</sup> bombardment. Also included in Fig. 5 are the absorbance corresponding to median-volume-con-

centration values induced by 1.0-, 2.0-, and 4.8-MeV Ne<sup>+</sup> irradiations.

In Fig. 5 we have also included the fast-neutron results of Chen *et al.*<sup>5</sup> for the 574-nm band. As the specific identity of this band had not been assigned nor its oscillator strength determined, Chen *et al.* presented their results in terms of absorption coefficient. Their  $\alpha$  scale is inserted on the left-hand side of the figure. Similarly, our ion results for the 574-nm band are presented in terms of absorbance. The ion-induced absorbance scales for both the 250- and 574-nm bands are inserted on the right-hand side.

We have found no relative change in the optical properties induced by MeV Ne<sup>+</sup> bombardment resulting from changes in the dose rate over a limited range explored. Samples were exposed to a total dose of  $10^{15}$  ions/cm<sup>2</sup> employing both 0.5- and 2.6- $\mu\text{A}$  3-MeV Ne<sup>+</sup> beams and the same absorption spectra and damage profiles were observed. This represented a dose rate range of  $0.7 \times 10^{12}$  to  $3.3 \times 10^{12}$  ions/cm<sup>2</sup> sec.

### C. $F$ -Type-Center Production Efficiency

Anion-sublattice-defect production in MgO is remarkably inefficient. Upon integration of the damage-profile results in Fig. 4 we find approxi-

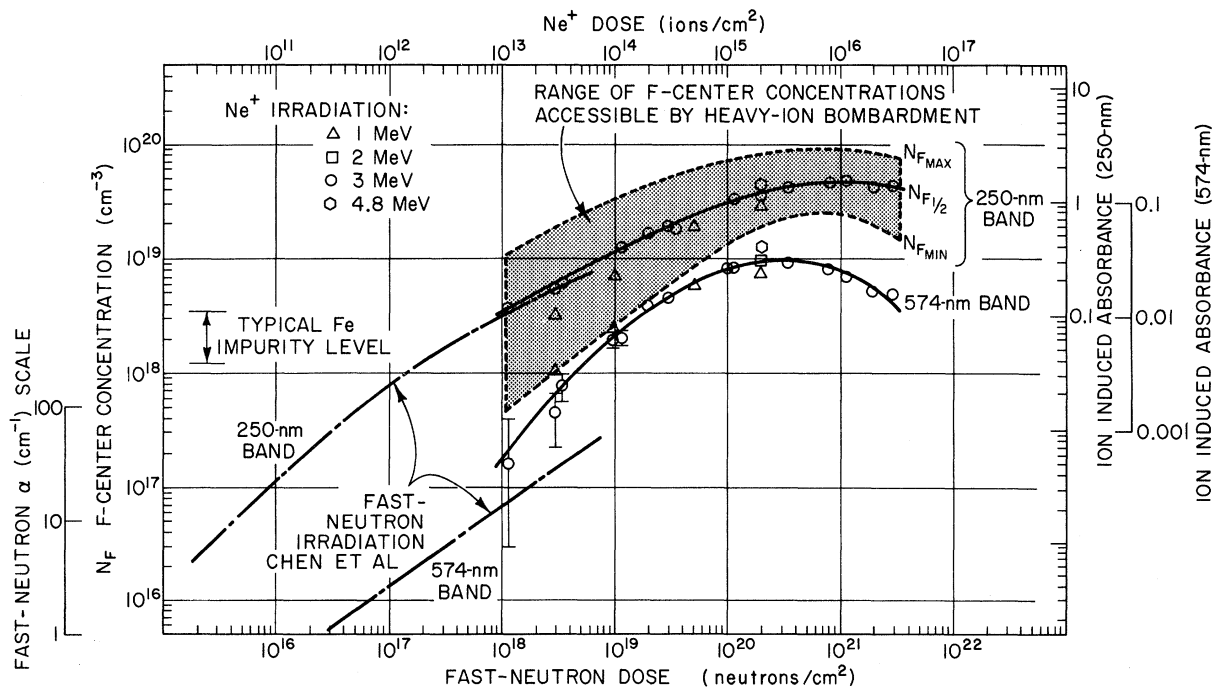


FIG. 5.  $F$ -type-center volume concentration induced in crystalline MgO by fast-neutron irradiation (results of Chen *et al.*) and by MeV  $^{20}\text{Ne}^+$  bombardment. The shaded region encloses a range of concentration resulting from a damage profile inherent with ion bombardment; the dot-dashed line obtained from the uniform spatial distribution of  $F$ -type centers induced by fast-neutron irradiation. The "equivalent" fast-neutron dose is approximately  $10^5$  times the Ne<sup>+</sup> dose (see Sec. II). Dose-vs-absorbance information for the 574-nm band is included. A typical transition-metal impurity level for the General Electric material is inserted on the left.  $N_{F_{\text{max}}}$  at saturation corresponds to about 1 in 600 anion sites converted to  $F$ -type centers.

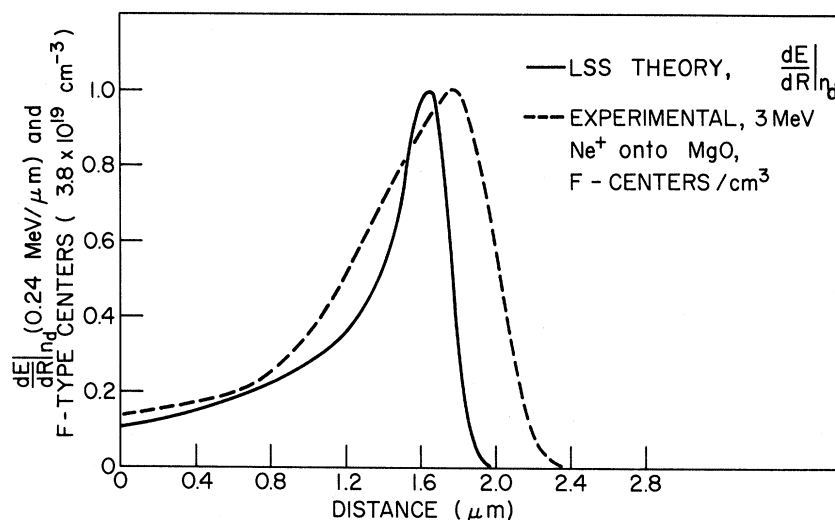


FIG. 6. A normalized comparison of nuclear stopping power predicted from LSS theory with the observed spatial distribution of the volume concentration of  $F$ -type centers. Both curves are for the case of 3-MeV  $\text{Ne}^+$  incident in MgO. The experimental dose was  $1 \times 10^{14}$  ions/cm<sup>2</sup>. The peak in stopping power occurs at 1.65  $\mu$ . This is within 7% of the observed damage profile peak at 1.77  $\mu$ . The observed damage profile full width at half-peak-height 0.83  $\mu$  is about twice the 0.40  $\mu$  range straggling predicted from LSS theory.

mately 30  $F$ -type centers are produced per incident 3-MeV ion; each center produced required some 100 keV. This very large energy per center suggests that an ionization mechanism (such as the Pooley-Hersh model)<sup>25,26</sup> must not be the dominant mode for producing defects. The probable mechanism is by atomic collisions, as we have assumed throughout. We compare the shape of the  $F$ -type-center volume-concentration profile (Fig. 4) with the spatial distribution of the distributed nuclear stopping power as predicted by LSS theory (Fig. 1). This comparison is shown in Fig. 6. The peak in stopping power occurs somewhat (about 7%) ahead of the damage-profile peak, and the observed damage-profile width is about twice the predicted range straggling. However, in view of the uncertainty of the accuracy of the LSS theory the overall agreement is rather striking. In view of the contrasting behavior of the ionization-loss curve  $(dE/dR)_e$  in Fig. 1, this strongly suggests that atomic collisions are primarily responsible for defect production on the MgO anion sublattice. This is in agreement with the conclusions drawn by Chen *et al.*<sup>16</sup> from their work on electron irradiated MgO.

The required formation energy per center may now be estimated assuming lattice defects are produced only by atomic collisions. Integrating the  $(dE/dR)_n$  curve in Fig. 1 and comparing with the incident energy we anticipate approximately 5% of the incident particle's energy should be deposited into the target by atomic collisions. Hence, at a dose of  $10^{14}$  ions/cm<sup>2</sup>, about 5 keV is required to produce each  $F$ -type center.

In making the normalized comparison shown in Fig. 6 we assume there is a constant ratio  $\beta$  between (a) the volume concentration of lattice defects anticipated on the basis of the predicted amount of energy deposited into the target per unit

volume by nuclear collisions at a given position  $x$  for a given threshold displacement energy, and (b) the observed volume concentration of  $F$ -type centers at  $x$ . The ratio  $\beta$  may be a function of many experimental variables such as dose, dose rate, target temperature, etc. It may be very difficult to derive  $\beta$  *a priori* assuming specific mechanisms operative. However, at a specific dose, dose rate, etc.,  $\beta$  may be estimated from our results. Assuming 5 keV per  $F$ -type center and a displacement threshold energy of 60 eV, we estimate  $\beta$  to be approximately eighty. This is similar to the situation in fast-neutron irradiated MgO near the equivalent dose. At a dose of  $5 \times 10^{18}$  neutrons/cm<sup>2</sup> about  $5 \times 10^{20}$   $F$ -type-centers/cm<sup>3</sup> are predicted.<sup>15</sup> Chen *et al.*<sup>5</sup> observed about  $7 \times 10^{18}$  cm<sup>-3</sup>, as indicated in Fig. 5. In that case  $\beta$  is about seventy. Of course for both cases, neutron and ion, we have neglected energy deposited through atomic collisions resulting in aggregate defects. This omission is small; as we suggest in Sec. IV, the concentration of a possible divacancy aggregate is low compared to the  $F$ -type-center concentration.

It is possible that there may be some anion vacancies which have not trapped electrons and would not be registered as  $F$ -type centers. To check this possibility, a sample previously exposed to a large 3-MeV  $\text{Ne}^+$  dose of  $1 \times 10^{16}$  ions/cm<sup>2</sup> was subsequently exposed to approximately  $10^6$  R  $\gamma$  irradiation from the NRL Co<sup>60</sup> source. There was no detectable change in the  $F$ -band intensity. This suggests that all anion vacancies were observed as  $F$ -type centers.

#### D. Annealing

Annealing studies of  $\text{Ne}^+$ -bombardment-induced lattice damage have been made. Isochronal annealing results for both the 250- and 574-nm band are

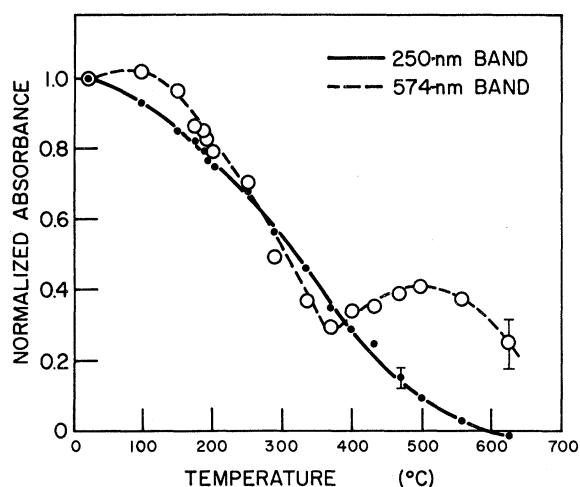


FIG. 7. Normalized isochronal anneal curves for both the 250- and 574-nm bands induced in MgO by 3-MeV  $\text{Ne}^+$  bombardment to a dose of  $3 \times 10^{14}$  ions/cm<sup>2</sup>.

shown in Fig. 7. Essentially all the  $F$ -type centers have been removed at 600 °C. This should be compared with some 1200 °C to remove the same band in additively colored MgO where, it is believed, only the vacancy is present to migrate.<sup>5</sup> This lower anneal value indicates that the annealing mechanism is probably the migration of the interstitial to the less mobile vacancy. These results are similar with those for fast-neutron irradiated MgO.<sup>5</sup> The initial 5% rise in the 574-nm band intensity near 100 °C is within the accumulated error of about  $\pm 7\%$  for these results. However, the substantial rise near 500 °C is real. In fact, a similar result has been reported<sup>5</sup> for the same band in fast-neutron irradiated MgO.

#### IV. DISCUSSION

The antimorph to the  $F^+$  center is the  $V^-$  center, a single hole trapped on an oxygen ion neighboring a cation vacancy.<sup>1</sup> This center has been associated with a broad ( $\Delta E \sim 1$  eV) absorption band near 2.3 eV.<sup>27</sup> Searle and Glass have examined the decay of the  $V^-$  center.<sup>28</sup> The center decays at room temperature with a half-life of 2 to 7 h. The hole is released from the center with an activation energy of  $1.13 \pm 0.05$  eV and may be subsequently trapped at an impurity such as  $\text{Fe}^{+2}$  or  $\text{Cr}^{+2}$  producing  $\text{Fe}^{+3}$  or  $\text{Cr}^{+3}$ . Sibley *et al.*<sup>29</sup> have associated a blue luminescence with the  $\text{Fe}^{+2} \rightarrow \text{Fe}^{+3}$  conversion, while Wertz *et al.*<sup>30</sup> have associated a red luminescence with a chromium trapping site.

We can make suggestive arguments as to why we do not observe the  $V^-$  band in Fig. 4 in spite of the fact that some of our measurements were taken within 30 min of removal from the Van de Graaff. First, separate calculations of the nuclear

stopping power for  $\text{Ne}^+$  incident on each of the MgO sublattices shows  $\text{Ne}^+$  has little preference for striking anions versus cations.<sup>31</sup> Second, a blue luminescence accompanied by a faint pink component was observed from the exposed portion of our MgO samples during bombardment. Third, ionization losses by the incident ions would have supplied more than enough energy to release trapped holes. And finally, as mentioned above, we did observe a growth of the  $\text{Fe}^{+3}$  absorption bands with bombardment dose. These four points suggest that vacancies may have been produced on the cation sublattice along with defects on the anion sublattice and that cation vacancies were simply not recorded by the presence of the  $V^-$  band because of impurity hole trapping. A possible mechanism for cation-vacancy destruction may be a sufficiently mobile cation interstitial near room temperature at which these irradiations were carried out.

In Fig. 5 the curve for 250-nm absorbance versus ion dose appears to decrease slightly above  $10^{16}$  ions/cm<sup>2</sup>. This effect is more obvious for the 574-nm band. For example, the absorbance of the 250-nm band at  $1.2 \times 10^{16}$  cm<sup>-2</sup> is  $1.54 \pm 0.01$  optical density (OD) while at  $2.0 \times 10^{16}$  cm<sup>-2</sup> it is  $1.40 \pm 0.01$  OD, representing a 9% absorbance decrease with an approximate twofold dose increase. This type of effect has also been observed for 3 MeV  $^{40}\text{Ar}$  bombarded LiF and for 60-keV  $^{14}\text{N}$  bombarded hexagonal SiC. For LiF a threefold increase in dose beyond the  $F$ -center saturation region causes a 7% decrease in the number of  $F$  centers produced.<sup>32</sup> The change in OD in hexagonal SiC resulting from the  $^{14}\text{N}$ -bombardment-induced lattice damage decreases by 8% for a 10-fold increase in dose.<sup>33</sup> This effect is not understood at this time.

Additive coloration, electron irradiation, and fast-neutron irradiation result in an intense 250-nm band. Other less intense bands near 355, 574, and 975 nm do not appear except with fast-neutron irradiation. Chen *et al.*<sup>5</sup> have suggested that these other bands may be associated with centers formed in a displacement spike<sup>34</sup> produced near the end path of a primary knock-on which had previously resulted from a collision with a fast neutron. Similar effects should be obtained from energetic ion bombardment. Our observation (see insert Fig. 2) of the 574-nm band supports this thesis. However, referring again to the insert Fig. 2, although the 574- and 355-nm bands are of comparable intensity in the neutron case, we do not observe the 355-nm band in the ion case. In fact  $\text{Ne}^+$  bombardment results in a proportionately larger 574-nm band. This can also be seen in Fig. 5 where a typical absorbance ratio OD (250)/OD (574) is 50% larger in the  $\text{Ne}^+$  case (at  $10^{15}$  ions/cm<sup>2</sup>) than the neutron case. As these are absorbance results they stand independent of any equivalent fast-neu-

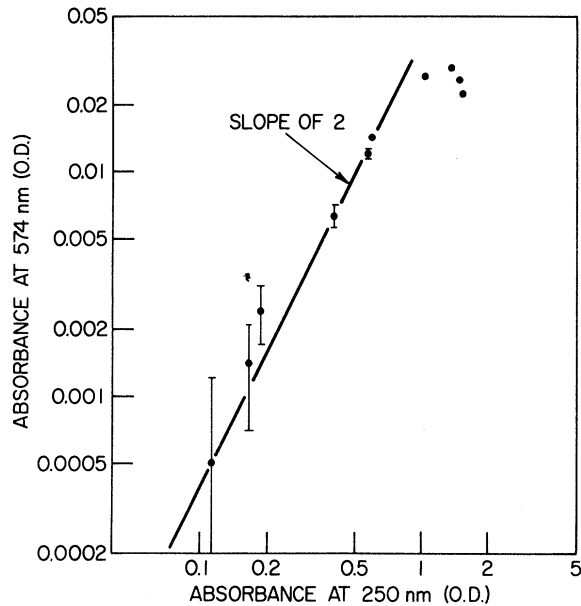


FIG. 8. Absorbance of the 574-nm band versus absorbance of the 250-nm band for 3-MeV  $\text{Ne}^+$  bombarded MgO.

tron dose arguments.

The 574-nm band may be associated with a multiple vacancy center. The most elementary such center is a divacancy, or an  $F_2$  center. Such  $F_2$  centers may be formed in the alkali halides by sufficient additive coloration or low-temperature irradiation. Assuming  $F$  centers are formed in a purely statistical manner,  $F_2$  centers appear when  $F$  centers are formed in sufficient concentration so that  $F$  centers may be formed at neighboring anion sites:

$$F_2 = (6/N_0)F^2, \quad (3)$$

where  $N_0$  is the density of anion sites. This naive approach neglects many possible effects such as the presence of an  $F$  center influencing the formation of a second  $F$  center at a neighboring anion site. However, if this approach is to be applicable anywhere, we expect it to be so in cases where the  $F$ - or  $F^+$ -center wave function is compact, such as in the host material MgO.<sup>35</sup> For our case, where the peak  $F$ -center concentration is near  $10^{20} \text{ cm}^{-3}$ ,  $10^{18} \text{ cm}^{-3}$   $F_2$ -type centers may be present. If the 574-nm band were to be associated with an  $F_2$ -like divacancy center we should expect from Eq. (3) the absorbance of this band to be proportional to the square of that of the 250-nm band if the oscillator strengths for these two centers were not concentration dependent. Figure 8 presents a comparison of data taken from Fig. 5 with the quadratic depen-

dence from Eq. (3). A straight line of slope 2 demonstrates how well the quadratic dependence is followed. The deviation at high concentrations occurs when both bands appear to saturate. The results in Fig. 8 then suggest that the 574-nm band may be associated with a divacancy.

As a consistency argument we may assume an oscillator strength  $F_{574}$  of 1.0 in Eq. (1) and compare the resulting concentration  $N_{F_2}$  predicted by Eq. (1) with that predicted by Eq. (3). The absorption coefficient  $\alpha_{\text{max}}$  is estimated by setting the effective thickness  $t = 2.3 \mu$ , where  $t$  is a measured value from profiles such as shown in Fig. 4. From Figs. 2 and 3 the absorption band full width at half-maximum  $\Delta E$  is approximately 0.25 eV. Equation (1) then predicts  $N_{F_2}$  to be about  $4 \times 10^{17} \text{ cm}^{-3}$ . From Fig. 5, at an ion dose of  $3.5 \times 10^{15}$  where the  $F$ -type-center median concentration  $N_{F_{1/2}}$  is about  $4.4 \times 10^{19} \text{ cm}^{-3}$ , Eq. (3) predicts about  $2 \times 10^{17} \text{ cm}^{-3}$   $F_2$ -like centers. The agreement is reasonable considering the approximations involved.

The presence of various electron traps provided by impurities represents a competing sink for electrons with the anion vacancies formed by ion bombardment. The maximum Fe impurity present in the General Electric MgO (see Table I) corresponds to a concentration of about  $7 \times 10^{18} \text{ cm}^{-3}$ , well below the  $F$ -type-center peak concentration near  $10^{20} \text{ cm}^{-3}$ . Other typical transition-metal impurities will be near or below this upper limit for iron. Therefore, the observed  $F$ -type-center saturation level is not believed to be governed by the presence of transition-metal impurities. As further support for this conclusion we have performed experiments similar to those leading to Fig. 5 employing ultra-high-purity MgO where the Fe impurity level was much lower, about  $1 \mu\text{g/g}$ .<sup>10</sup> In this case the observed saturation level was the same. Other transition-metal impurities such as Ti, Mn, and Cu were known to be present at a much higher level in the General Electric MgO than in the Oak Ridge material but did not observably alter the  $F$ -type-center saturation level. In addition, the observed saturation level for the 574-nm band was similarly unchanged in the ultra-high-purity material.

#### ACKNOWLEDGMENTS

One of the authors (B. D. E.) would like to thank Dr. V. H. Ritz for his many helpful comments and suggestions and Dr. F. L. Carter and members of the Central Materials Research Activity for the crystallographic direction measurements and sample preparations. We are indebted to Dr. M. N. Kabler and Dr. C. C. Klick for critical discussions.

<sup>1</sup>A. E. Hughes and B. Henderson, Atomic Energy Research Establishment (Harwell) Report No. AERE-

R6582, 1970 (unpublished).

<sup>2</sup>B. Henderson and J. E. Wertz, *Advan. Phys.* **17**,

747 (1968).

<sup>3</sup>E. Sonder and W. A. Sibley, *Defects in Solids*, edited by J. H. Crawford and L. Slifkin (Plenum, New York, to be published).

<sup>4</sup>Lawrence A. Kappers, Roger L. Kroes, and Eugene B. Hensley, *Phys. Rev. B* 1, 4151 (1970).

<sup>5</sup>Y. Chen, R. T. Williams, and W. A. Sibley, *Phys. Rev.* 182, 960 (1969).

<sup>6</sup>B. Henderson and R. D. King, *Phil. Mag.* 13, 1149 (1966).

<sup>7</sup>J. Lindhard, M. Scharff, and H. E. Schiott, *Kgl. Danske Videnskab. Selskab, Mat. Fys. Medd.* 33, No. 14 (1963).

<sup>8</sup>Obtained from the General Electric Co., Cleveland, Ohio through the cooperation of Dr. L. J. Schupp.

<sup>9</sup>Obtained from the Oak Ridge National Laboratory, Research Materials Program, Solid State Division, through the cooperation of Dr. John W. Cleland and Dr. Ed Sonder.

<sup>10</sup>C. T. Butler, B. J. Sturm, and R. B. Quincey, Jr., Oak Ridge National Laboratory Report No. ORNL-4547 (unpublished).

<sup>11</sup>T. K. Ghosh and F. J. P. Clarke, *Brit. J. Appl. Phys.* 12, 44 (1961).

<sup>12</sup>S. Tolansky, *Multiple-Beam Interferometry of Surfaces and Films* (Clarendon, London, 1948).

<sup>13</sup>D. L. Dexter, *Solid State Phys.* 6, 353 (1958).

<sup>14</sup>G. L. Kulcinski, J. J. Laidler, and D. G. Doran, *Radiation Effects* 7, 195 (1971).

<sup>15</sup>G. H. Kinchin and R. S. Pease, *Rept. Progr. Phys.* 18, 1 (1955).

<sup>16</sup>Y. Chen, D. L. Trueblood, O. E. Schow, and H. T. Tohver, *J. Phys. C* 3, 2501 (1970).

<sup>17</sup>Reference 14, Eq. (8).

<sup>18</sup>Extended to higher energies and other combinations

of beam and target by E. A. Wolicki (private communication).

<sup>19</sup>William S. Johnson and James F. Gibbons, *Projected Damage Statistics in Semiconductors* (distributed by Stanford University Bookstore, 1969).

<sup>20</sup>R. W. Soshea, A. J. Dekker, and J. P. Sturtz, *J. Phys. Chem. Solids* 5, 23 (1958).

<sup>21</sup>Jack C. Cheng and James C. Kemp, *Phys. Rev. B* 4, 2841 (1971).

<sup>22</sup>Y. Chen and W. A. Sibley, *Phil. Mag.* 20, 217 (1969).

<sup>23</sup>R. D. King and B. Henderson, *Proc. Phys. Soc. (London)* 89, 153 (1966).

<sup>24</sup>James A. Glaze and James C. Kemp, *Phys. Rev.* 170, 1502 (1969); 170, 1507 (1969).

<sup>25</sup>D. Pooley, *Solid State Commun.* 3, 241 (1965).

<sup>26</sup>H. N. Hersh, *Phys. Rev.* 148, 928 (1966).

<sup>27</sup>Y. Chen and W. A. Sibley, *Phys. Rev.* 154, 842 (1967).

<sup>28</sup>T. M. Searle and A. M. Glass, *J. Phys. Chem. Solids* 29, 609 (1968).

<sup>29</sup>W. A. Sibley, J. L. Kolopus, and W. C. Mallard, *Phys. Status Solidi* 31, 223 (1969).

<sup>30</sup>J. E. Wertz, L. C. Hall, J. Halgeson, C. C. Chao, and W. S. Dykoski, *Interaction of Radiation with Solids*, edited by A. Bishay (Plenum, New York, 1967), p. 617.

<sup>31</sup>I. Manning (private communication).

<sup>32</sup>K. L. Vander Lugt, J. Comas, and E. A. Wolicki, *J. Phys. Chem. Solids* 31, 1361 (1970).

<sup>33</sup>A. Addamiano, G. W. Anderson, W. Lucke, and J. Comas, *J. Electrochem. Soc.* 118, 291C (1971).

<sup>34</sup>John A. Brirkman, *J. Appl. Phys.* 25, 961 (1954).

<sup>35</sup>James C. Kemp and Victor I. Neeley, *Phys. Rev.* 132, 215 (1963).